URTeC: 2457581

Benchmarking Recovery Factors of Individual Wells Using a Probabilistic Model of Original Gas in Place to Pinpoint the Good, Bad and Ugly Producers

John Richardson*, Wei Yu, Ruud Weijermars, Texas A&M University

Copyright 2016, Unconventional Resources Technology Conference (URTeC) **2457581**

This paper was prepared for presentation at the Unconventional Resources Technology Conference held in San Antonio, Texas, USA, 1-3 August 2016.

The URTeC Technical Program Committee accepted this presentation on the basis of information contained in an abstract submitted by the author(s). The contents of this paper have not been reviewed by URTeC and URTeC does not warrant the accuracy, reliability, or timeliness of any information herein. All information is the responsibility of, and, is subject to corrections by the author(s). Any person or entity that relies on any information obtained from this paper does so at their own risk. The information herein does not necessarily reflect any position of URTeC. Any reproduction, distribution, or storage of any part of this paper without the written consent of URTeC is prohibited.

Summary

Estimation of original gas in place (OGIP) in a rock volume provides an upper limit for the expected ultimate recovery. Calculation of OGIP for a drainage region may introduce significant errors when based on discrete values; the deterministic OGIP may be either overestimated (positively biased) or underestimated (negatively biased). For example, parameters like porosity, water saturation and adsorbed gas density may vary spatially, which must be accounted for to obtain realistic OGIP estimations.

Our objective was to create a more accurate OGIP model and use it to probabilistically asses OGIP, estimated ultimate recovery (EUR) and recovery factor (RF) for shale gas reservoirs like the Marcellus shale. The conventional OGIP model was updated to include recent developments in shale geology and gas adsorption. Corrections to traditional free gas calculations are made by subtracting adsorbed gas reservoir volume from free gas volume in order to obtain improved OGIP estimations. This change was assessed in the context of Langmuir and BET isotherm adsorption models. A 25-year EUR response surface model was created using a semi-analytical model from our previous work. Both OGIP and EUR models were coupled during Monte Carlo simulation to produce a probability distribution for RF.

When adsorbed gas was included in the pore space available for free gas, OGIP for the Marcellus was reduced 14% from previous estimates. With this model, changing from the traditional Langmuir isotherm to a BET isotherm resulted in a marginal gains in OGIP. Using the limited tuning parameters available for the BET isotherm, a 14-24% reduction in Marcellus OGIP was observed. The coupled OGIP-EUR simulation produced a P50 OGIP estimate of 1,320 Tcf, P50 EUR of 492 Tcf, and P50 RF of 38%.

Introduction

Estimated ultimate recovery (EUR) when divided by original gas in place (OGIP) produces a recovery factor (RF). Technically recoverable resources (TRR) is the portion of OGIP that can be recovered with current technology, EUR is the subset of TRR that is economically recoverable. Global assessment of unconventional gas resources has recently been progressing toward probabilistic modeling of EUR/TRR, OGIP and RF. Compared to deterministic methods, probabilistic modeling captures the variability of geological factors and quantifies the uncertainty in estimates making it a superior method.

Dong (2012) developed the Unconventional Gas Resource Assessment System (UGRAS) to determine probabilistic OGIP, TRR and RF. Her dissertation was a landmark study in global resource assessment and was the first large scale probabilistic modeling of unconventional resources. Of particular interest is the assessment of five major US shale gas

plays, the Barnett, Eagle Ford, Marcellus, Fayetteville and Haynesville Shale. The model of OGIP used by Dong (2012) needs updating with new developments in understanding of shale geology and gas adsorption behavior.

Shales are fine-grained organic-rich sedimentary rocks which serve as both a source rock and reservoir for hydrocarbons. Shale gas, a natural gas mainly composed of methane, is primarily associated with the organic rich portions of the reservoir. The gas in shales exists in two states, adsorbed and free. Free gas occupies small nanopores within the shale, and adsorbed gas is associated with the organics in the rock. Although models of OGIP do include the volume of adsorbed gas they do not consider it to be in competition with the pore space occupied by free gas.

The interconnected pore space within the shale is dependent on the organics (Wang 2009; Loucks et al. 2009; Sondergeld et al 2010). Ambrose et al. (2012) investigated this dependency in kerogen containing shales and concluded the organic material composes a majority of pore volume occupied by gas. Dong (2012) assumed that there is no competition for pore space which is incorrect when the organic material to which gas adsorbs also creates the pore space (Ambrose et al 2012). Not only is it incorrect, adsorbed gas occupied a *significant* portion of pore volume otherwise available to free gas. Importantly, the result is a reduction of the pore space available to free gas and the net impact on OGIP due to the competition for space between adsorbed and free gas is investigated and quantified in our study.

Regardless of the adsorbed gas competing with free gas for pore space, the adsorption behavior is usually modeled with a single-layer Langmuir isotherm (e.g. Ambrose et al. 2012; Alnoaimi and Kovscek 2013; Naraghi and Javadpour 2015; Jin and Firoozabadi 2016). This method has since been further improved by Yu et al. (2014) who analyzed the dependence of gas storage capacity on pressure in four samples of Marcellus shale and from this data discovered that gas desorption was better modeled by a multi-layer BET isotherm (Brunauer et al. 1938) rather than the traditional single-layer Langmuir isotherm (Langmuir 1918) used by Dong (2012). Notably, Yu et al. (2014) determined gas storage capacity at pressures up to 7,500 psi. Fitting a model to the adsorption behavior at sub-3000 psi conditions can be misleading because storage capacity did not significantly differ from that of a single-layer isotherm until pressure exceeded 3000 psi (Yu et al. 2014). It is possible that past studies (e.g. Alnoaimi and Kovscek 2013; Jin and Firoozabadi 2016) have correctly modeled sub-3000 psi adsorption behavior with a Langmuir isotherm, but may fall short of describing adsorption behavior at known reservoir conditions, which may exceed 3000 psi.

Gas in the adsorbed phase is denser than free gas, thus if more layers of gas are added at the expense of free-gas pore space, OGIP will increase. Modeling of adsorbed gas as a multi-layer system increases OGIP estimates when compared to the single-layer case. Pore space sharing by gas phases and the change from a Langmuir to BET isotherm have significant effects on OGIP (**Figure 1**). Yu et al. (2014) did consider pore space competition between gas phases, but only used discrete values when evaluating the influence of the BET isotherm on OGIP.

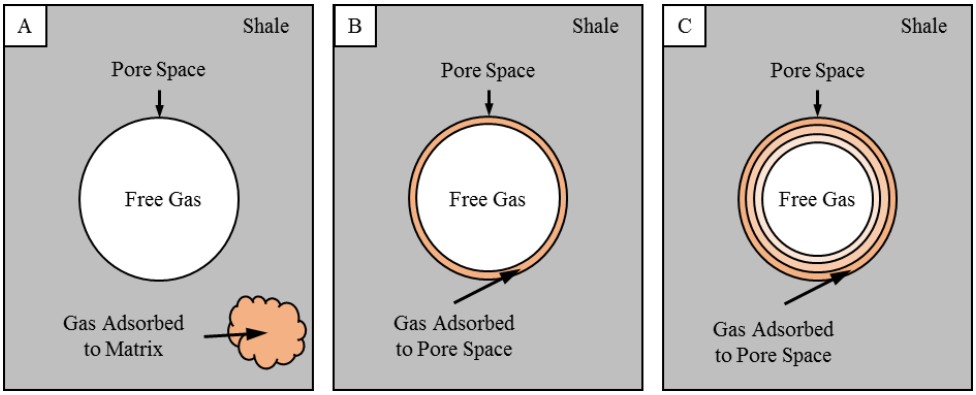

Figure 1. Diagram of adsorbed gas not in competition with the pore space available for free gas (A). Langmuir isotherm behavior of adsorbed gas in competition for pore space with free gas (B). BET isotherm behavior showing multiple layers of adsorbed gas in competition with pore space (C). Color intensity of adsorbed layer is meant to indicate higher density values adsorbed gas.

Dong et al. (2015) summarize probability density distributions for most input parameters used in the OGIP model. However, the latter study accounts for gas adsorption behavior with a single-layer Langmuir isotherm without subtracting the volume occupied by adsorbed gas from the free gas volume, which overestimates OGIP as can be concluded from our results reported below. The effect of reduced free gas pore space and multi-layer adsorption modeling on these previously published region-scale estimates is assessed in the present study. The need for updated OGIP and estimate methodology is paramount for assessing the good, bad and ugly well performers.

OGIP Model

OGIP is calculated as a sum of free gas volume (V_f) and adsorbed gas volume (V_a) in standard cubic feet (scf):

$$OGIP = V_f + V_a \quad . \tag{1}$$

Adsorbed Gas Volume. Drainage area (A) in acres, pay zone height (h) in feet, and bulk rock density (ρ_b) in gram per cubic centimeter are multiplied by the standard volume (standard cubic feet) of gas per ton of rock (v_a) to obtain the volume (scf) of adsorbed gas in place (V_a):

$$V_a = 1359.7\, A\, h\, \rho_b v_a \quad . \tag{2}$$

Adsorbed gas per ton of rock, also known as storage capacity, when calculated from the Langmuir isotherm (Langmuir 1918) (v_{a_Lang}) is a function of Langmuir volume (V_L), Langmuir pressure (P_L) and pressure:

$$v_{a\_Lang} = V_L \left(\frac{P}{P + P_L}\right) \quad . \tag{3}$$

Eq. (3) is valid for any consistent pressure units, and depends on the units V_L which are scf/ton in this model. With recent developments indicating that that adsorbed gas behavior is well described by a BET isotherm (Yu et al. 2014), v_a may be better calculated by the BET model in some locations:

$$v_{a\_BET} = \frac{v_m\, C \left(\frac{P}{P_0}\right)}{\left(1 - \frac{P}{P_0}\right)} \left\{ \frac{1 - (n+1)\left(\frac{P}{P_0}\right)^n + n\left(\frac{P}{P_0}\right)^{n+1}}{1 + (C-1)\frac{P}{P_0} - C\left(\frac{P}{P_0}\right)^{n+1}} \right\} \quad , \tag{4}$$

where C is a unitless constant related to net heat of adsorption, v_m is the maximum volume of a unimolecular layer of gas and n is the maximum number of adsorbed layers. The units of v_{a_BET} may either be standard cubic feet of adsorbed gas per ton of bulk rock (scf/ton) or standard cubic centimeters per gram of rock. The units of v_{a_BET} should match the units of v_m. To stay consistent with field units, scf/ton is used.

The saturation pressure, P_0, loses meaning at supercritical conditions existing in the reservoir (Ozdemir 2004). To remedy this, Yu et al. (2014) used a correlation established by Clarkson et al. (1997) to calculate pseudosaturation pressure as a function of temperature:

$$ln(P_s) = 7.7437 - \frac{1306.5485}{19.4362 + T} \quad , \tag{5}$$

where P_s is the pseudosaturation pressure (MPa) and T is temperature (K). Gas storage capacity can be calculated by either model and substituted into v_a in Eq. (2).

Free Gas Volume. The basic equation for calculating free gas volume (V_f) is:

$$V_f = 43560 \frac{A\, h\, \phi_m (1 - S_{wm})}{B_g} \quad , \tag{6}$$

where ϕ_m is the fractional matrix porosity, S_{wm} is the fractional matrix water saturation and B_g is the formation volume factor of the free gas in rcf/scf. Area (A) is in acres and pay zone height (h) is in feet. In a matrix with fractures two different water saturation level exist, one for the matrix (S_{wm}) and another for the fracture (S_{wfrac}). Fracture porosity is added to Eq. (6) with a separate water saturation for each porosity.

$$V_f = 43560 \frac{A\, h \left[\phi_m (1 - S_{wm}) + \phi_{frac} \left(1 - S_{wfrac}\right)\right]}{B_g} \quad , \tag{7}$$

where matrix porosity (ϕ_m) and fracture porosity (ϕ_{frac}) can be calculated if the storativity ratio (ω) of the rock and bulk porosity (ϕ_b) are known:

$$\omega = \frac{\phi_{frac}\, c_{frac}}{\phi_{frac}\, c_{frac} + \phi_m\, c_m} \quad , \tag{8}$$

$$\omega = \frac{\phi_{frac}}{\phi_{frac} + \phi_m} = \frac{\phi_{frac}}{\phi_b} \quad . \tag{9}$$

Eq. (8) reduces to Eq. (9) if one assumes that fracture and pore space compressibility are approximately equal, as commonly applied in previous studies (Wang 2014; Bahrami et al. 2012). The net void space of the rock after accounting for matrix and fracture porosity and their corresponding water saturations is typically used to estimate the volume occupied by free gas. This assumption was shown to be incorrect by Ambrose et al. (2012) who instead showed adsorbed gas and free gas compete for pore space. To compute the free gas volume correctly, pore space available to free gas should take into account the reduction of pore space attributable to adsorbed gas (ϕ_a).

$$V_f = 43560 \frac{A\, h \left[\phi_m (1 - S_{wm}) + \phi_f \left(1 - S_{wf}\right) - \phi_a\right]}{B_g} \quad . \tag{10}$$

Pore space occupied by the adsorbed gas (ϕ_a) is defined in terms of the volume of adsorbed gas (v_a), adsorbed gas density (ρ_a), bulk rock density (ρ_b), and molecular weight (M) (Ambrose et al. 2012):

$$\phi_a = 1.318 \times 10^{-6} M \frac{\rho_b}{\rho_a} v_a \quad . \tag{11}$$

In Eq. (11), the molecular weight (M) of the gas in lbm/lbmol was calculated from a constant specific gravity for the reservoir. Combining Eqs. (1), (2), (10) and (11), a formula for OGIP is obtained:

$$OGIP = 43560 \frac{A\, h \left[\phi_m (1 - S_{wm}) + \phi_f \left(1 - S_{wf}\right) - 1.318 \times 10^{-6} M \frac{\rho_b}{\rho_a} v_a\right]}{B_g} + 1359.7\, A\, h\, \rho_b v_a \quad , \tag{12}$$

where v_a can be estimated by either the BET or Langmuir isotherm, and porosity available for free gas has been reduced by the porosity occupied by the adsorbed gas has. Water fractions S_{wm} and S_{wf} are for the matrix and fracture respectively.

Formation volume factor (B_g) was calculated as a function of pressure and temperature at reservoir conditions (P, T) and standard conditions (P_{sc} , T_{sc}) and adjusted by Z factor:

$$B_g = Z \frac{T\, P_{sc}}{P\, T_{sc}} \quad . \tag{13}$$

Eq. (13) works for any consistent unit of temperature and pressure, in this study degrees Rankine and psi were used. Z factor tables were generated by a visual basic program using the iterative method outlined by (Abou-Kassem et al. 1990) for calculating natural gas Z factor. The Z factor value used in Eq. (13) was interpolated from the generated table.

In addition to B_g, adsorbed gas density (ρ_a) in Eq. (12) is also a function of the pressure. Riewchotisakul and Akkutlu (2015) used nonequilibrium molecular dynamic simulations to create an equation calculating adsorbed methane density (ρ_a in g/cc) in organic pore spaces based on pressure in psi. Although the gas in shales is not entirely methane, an assumption was made that this function would be sufficient for modeling purposes:

$$\rho_a = 0.1057 \ln(P) - 0.4629 \quad . \tag{14}$$

For matrix and fracture modeling, it was assumed that the distribution of porosity and water saturation both followed the partitioning determined by the storativity ratio.

$$\omega = \frac{\phi_f}{\phi_f + \phi_m} = \frac{S_{wf}}{S_{wf} + S_{wm}} \quad . \tag{15}$$

Semi-analytical Model

A semi-analytical model was used to accurately predict the EUR in shale gas reservoirs with multiple hydraulic fractures (**Figure 2**). Hydraulic fractures were discretized into fracture segments by the semi-analytical model. Spatial and temporal superposition was used to take into account the interaction of fracture segments. The semi-analytical model primarily contains two parts, an analytical plane-source solution used to solve the diffusivity equation of gas flow from shale to each fracture segment and a numerical solution used to solve gas flow along fracture segments. The model considers multiple gas transport mechanisms including gas desorption (Langmuir and BET isotherms), gas slippage, gas diffusion, and non-Darcy flow. The nonlinear diffusivity equation for gas flow from shale into fractures under the condition of residual water saturation is given by:

$$\nabla \cdot \left\{ \left[\frac{\rho_g k \, (1 + 8\alpha K_n)}{\mu_g} + \frac{\delta}{\tau} \phi_b D_g \rho_g c_g S_g \right] \nabla P \right\} = \left[S_g \phi_b + (1 - \phi_b) K_a \right] c_g \rho_g \, \frac{\partial P}{\partial t} \quad , \tag{16}$$

where ρ_g is gas density, k is reservoir permeability, μ_g is gas viscosity, α is a constant and close to 1, K_n is Knudsen number, D_g is Fickian diffusivity of gas component through the pore, δ is a dimensionless constrictivity factor, τ is dimensionless tortuosity, c_g is the isothermal gas compressibility factor, S_g is gas saturation (1 - S_w), K_a is the differential equilibrium partitioning coefficient of gas at a constant temperature, which is function of pressure and temperature and defined as (Cui et al., 2009; Patzek et al., 2013):

$$K_a = \left(\frac{\partial \rho_a}{\partial \rho_g} \right)_T = \frac{\rho_g(P_{ST}, T_{ST}) \, \rho_b}{1 - \phi_b} \frac{\partial v_a}{\partial P} \, \frac{\partial P}{\rho_g} \quad , \tag{17}$$

where ρ_g (P_{ST}, T_{ST}) is the stock tank gas density, ρ_b is bulk density of shale, v_a is the specific volume of gas adsorbed per unit mass of bulk rock (scf/ton). For the Langmuir isotherm, the differential equilibrium partitioning coefficient is expressed as follows:

$$K_a = \frac{\rho_g(P_{ST}, T_{ST}) \, \rho_b}{(1 - \phi_b) c_g \rho_g} \, \frac{V_L P_L}{(P + P_L)^2} \quad . \tag{18}$$

For the BET isotherm, the differential equilibrium partitioning coefficient of gas is calculated by:

$$K_a = \frac{\rho_g(P_{ST}, T_{ST}) \, \rho_b}{(1 - \phi_b) c_g \rho_g} \, \frac{v_a^2}{C v_m P_o} \left(\frac{P_o^2}{P^2} + C - 1 \right) \quad . \tag{19}$$

For gas flow along the fractures, the non-Darcy flow is considered and modeled:

$$-\nabla P = \frac{\mu_g}{k} v_g + \beta \rho_g v_g^2 \quad , \tag{20}$$

where v_g is gas velocity, β is the non-Darcy Forchheimer coefficient which can be calculated using the correlation proposed by Evans and Civan (1994).

More details about the model development, solution, and verification can be found in previous studies (Yu 2015; Yu et al. 2015).

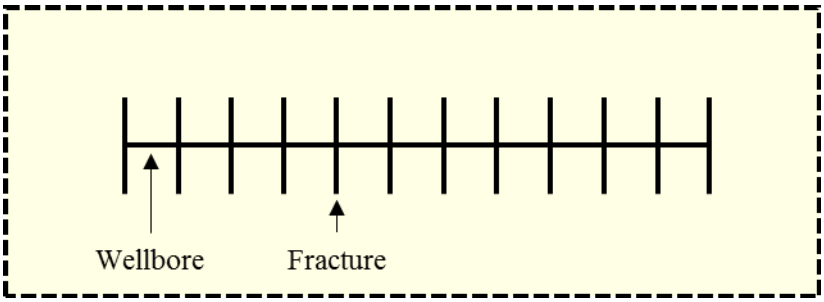

Figure 2. Well and drainage region geometry used in the semi-analytical model.

Response Surface Methodology

In order to build the correlation between the EUR and uncertain reservoir and fracture variables, an efficient statistical technique of Response Surface Methodology (RSM) is used. A full quadratic polynomial model in the RSM is expressed below:

$$y = \beta_o + \beta_1 x_1 + \beta_2 x_2 + \cdots + \beta_k x_k + \sum_{i<j}^{k} \sum_{=2} \beta_{ij} x_i x_j + \sum_{i=1}^{k} \beta_{ii} x_i^2 + \varepsilon \quad , \tag{21}$$

where y is the objective function (for example, EUR), x_i (i = 1, …, k) are uncertain variables, β_i (i = 1, …, k) are regression coefficients, k is the number of uncertain variables investigated, and ε is the error term.

The approach of D-optimal design is often used to fit the quadratic polynomial model (Yu and Sepehrnoori 2014). More detailed mathematical and statistical theories of D-optimal design can be found in the work by Myers et al. (2008). After obtaining the polynomial model as a proxy model, we can predict the EUR at any points in the uncertain parameter space. Furthermore, we can combine the proxy model and Monte Carlo method to explore the probabilistic distribution of EUR (for example, P10, P50, and P90) through generating a large number of samples.

Probabilistic Modeling

Probabilistic calculations were performed with the plugin @Risk in conjunction with Excel. @Risk uses Monte Carlo simulation with a range of sampling methods to select for each input parameter an established uncertainty range including the probability defined for the occurrence of each specific the value in that range. Each simulation ran 100,000 iterations for statistical significance and convergence of the resulting gas volume probability distributions. Most parameters in Eq. (12) can be represented as probability distributions either explicitly or implicitly through other variables (like B_g depending on pressure). Parameters with associated distributions were net pay, pressure, permeability, porosity, and water saturation. We did not consider reduction in uncertainty due to correlated distributions, which may be scope for further study. Static and probabilistic reservoir parameters used for the Marcellus shale by Dong et al. (2015) are listed in **Tables 1** and **2** respectively. The static parameters were area, temperature, bulk rock density, storativity ratio, specific gravity of the gas, and isotherm tuning parameters. The value

of specific gravity used by Dong et al. (2015) was used in this study (and confirmed in personal communications with the latter principal author).

The application of both Langmuir and BET isotherm tuning parameters is problematic. There is no known method available for validating their application to a spatial region, neither exists a generally accepted procedure to apply such parameters probabilistically. For this reason, the tuning parameters for BET and Langmuir isotherms were applied as static values (**Table 3**). Langmuir data was included in Dong et al. (2015), but BET isotherm parameters are largely missing from literature.

Yu et al. (2014) obtained BET tuning parameters (v_m, n and C) from four experiments with Marcellus shale cores. For each shale core sample, Yu et al. (2014) had a set of BET and Langmuir tuning parameters fit to the data. The Langmuir data published by Dong et al. (2015) cannot be directly compared to the BET data from Yu et al. (2014) because the tuning parameters are not attempting to describe the same behavior. For a direct comparison of changing isotherm models, the Langmuir and BET isotherm tuning parameter pairs from Yu et al. (2014) were used. Workflow for models and application of probabilistic inputs is presented in **Figure 3**.

Input	Marcellus
Area (acres)	640
Temperature (˚R)	595
Bulk Rock Density (g/cc)	2.5
Storativity Ratio	0.1
Specific Gravity	0.6

Table 1. Static values (Dong et al. 2015) used to calculate gas volumes and production forecasts.

Input	Marcellus
Net Pay (ft)	GEV[a] (120, 70, 0.1)
Initial Pressure (psi)	Triangular[b] (2,000, 4,100, 5,100)
Permeability (md)	Log-normal[c] (0.0003, 0.0002)
Porosity (fraction)	Gamma[d] [4, 0.007, Shift(0.03)]
Bulk Water Saturation (fraction)	Normal (0.26, 0.08)

[a] GEV (mean, standard deviation, shape parameter) Generalized Extreme Value
[b] Triangular (min, most likely, max)
[c] Log-normal (mean, standard deviation)
[d] Gamma (shape parameter, scale parameter)

Table 2. Distribution functions (Dong et al. 2015) used to calculate gas volumes and production forecasts.

		Sample 1[a]		Sample 2		Sample 3		Sample 4		Literature[b]
Adsorption Model		Langmuir	BET	Langmuir	BET	Langmuir	BET	Langmuir	BET	Langmuir
Adsorbed Gas (Bcf/section)	P90	23	27	16	16	10	11	6	6	11
	P50	54	64	38	37	24	25	13	14	26
	P10	103	123	72	71	46	49	25	27	49
Free Gas (Bcf/section)	P90	4	1	8	8	11	11	14	13	11
	P50	16	11	23	24	30	29	35	34	29
	P10	44	36	56	57	67	66	76	75	66
OGIP (Bcf/section)	P90	30	32	26	26	23	23	20	20	23
	P50	72	77	63	62	55	55	49	49	56
	P10	142	153	125	125	112	113	100	101	113

[a] Samples 1-4 isotherm tuning parameters from Yu et al. 2014.
[b] Literature values from Dong et al. 2015.

Table 3. BET and Langmuir isotherm tuning parameters used as static values in probabilistic modeling.

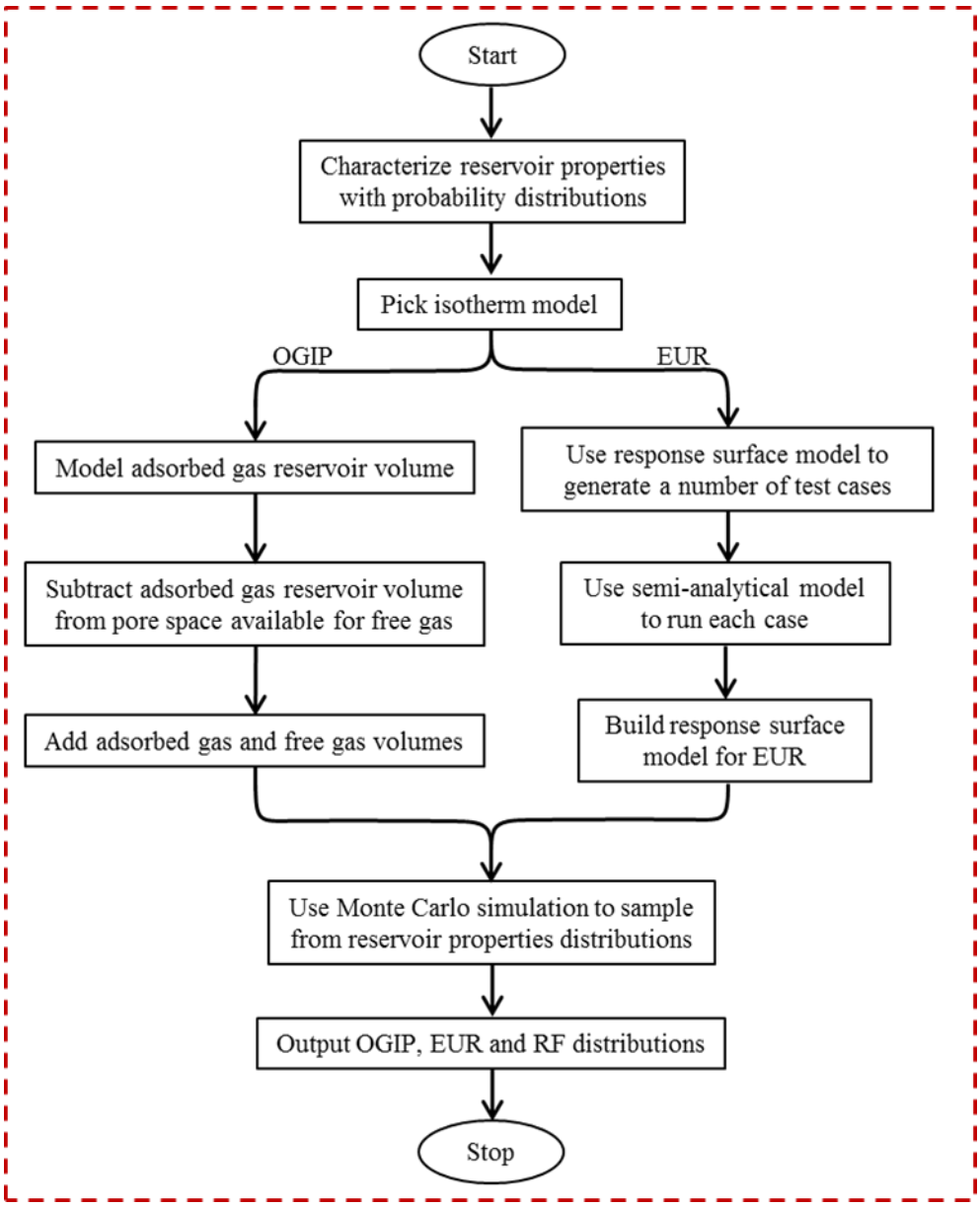

Figure 3. Workflow used to generate OGIP, EUR and RF distributions for the Marcellus shale in this case study.

Case Study

OGIP Prediction. To assess the effects of the OGIP model developed, pore space competition and isotherm models were added in steps. The probabilistic gas volumes for the Marcellus are compared for each major change in the model. The conventional case (Case 1) assumes a Langmuir isotherm model of adsorbed gas volume, and incorrectly assumes adsorbed gas not co-occupying pore space with free gas (Figure 1A). The first modification (Case 2) includes adsorbed gas in the pore space rather than on the matrix, consequently reducing pore volume available for free gas (Figure 1B). The second modification (Case 3) models adsorbed gas volume within the pore space with a BET isotherm (Figure 1C). In each case, a distribution for adsorbed gas, free gas and OGIP was generated (**Figure 4**). From these distributions, the P10, P50, and P90 values were extracted such that the P90 means 90% of wells would be expected to have values greater than the one listed (**Table 4**). It is important to note that the adsorbed gas P50 and free

gas P50 will not always sum to the OGIP P50, because medians are not inherently additive like mean values. The same principle is true for P10 and P90 values.

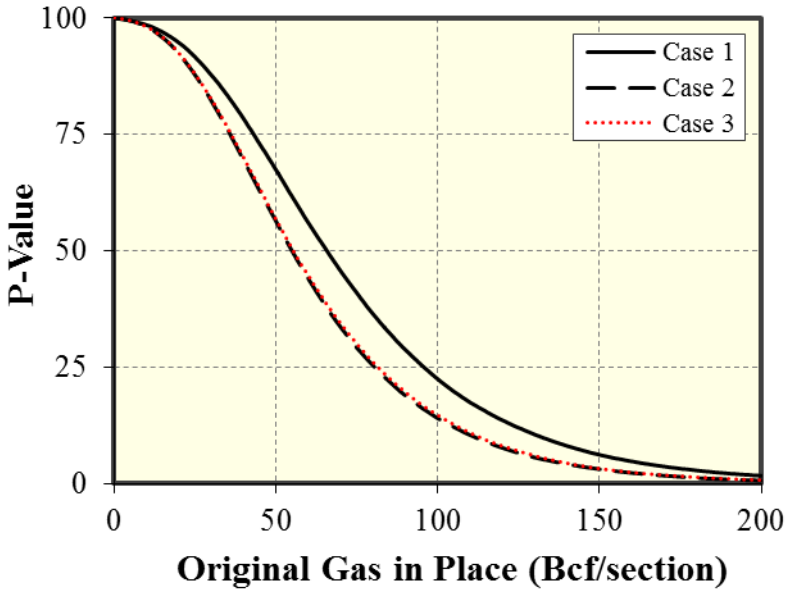

Figure 4. Comparison between key model changes. Case 1 used Langmuir modeling of gas adsorption to the rock matrix. Case 2 used the same Langmuir isotherm model as Case 1, but gas was adsorbed inside the pore space, reducing pore volume available for free gas. Case 3 included both a BET isotherm model and reduction of free gas by gas adsorption.

		Case 1	Case 2	Case 3
Adsorbed Gas (Bcf/section)	P90	10.4	10.4	10.8
	P50	24.3	24.3	25.4
	P10	46.3	46.3	49.1
Free Gas (Bcf/section)	P90	16.2	11.2	11.0
	P50	40.9	29.8	29.1
	P10	87.0	67.2	65.9
OGIP (Bcf/section)	P90	27.3	22.5	22.7
	P50	65.8	54.9	55.3
	P10	132.1	111.5	113.0

Table 4. Comparison between key model changes presented in Figure 4. P-Value of adsorbed gas volume, free gas volume and OGIP are based on probabilistic inputs and represent the P90, P50, and P10 output of the model.

The data in Figure 4 and the accompanying Table 4 was generated using probabilistic data from Table 2, static parameters from Table 2 and Sample 3 gas adsorption tuning parameters from Table 3. When this analysis was rerun using the Langmuir tuning parameters from Dong et al. (2015), the OGIP P50 changed from 67.2 (Case 1) to 55.6 Bcf/ton (Case 2). A recreation of the model used by Dong et al. (2015) as well as OGIP distributions for shale plays presented in the paper is presented in **Appendix A**.

Generally, the change to a BET isotherm results in an OGIP value that is approximately equal to or greater than the Langmuir isotherm (**Table 5**). The magnitude of this change in the P50 region ranged from -0.6 to 5.0 Bcf per section. The maximum effect of changing models is a 10.2 Bcf increase in the P10 values of sample 1. The increase in OGIP is from the adsorbed gas phase, which is greater than the reduction of free gas volume induced by changing adsorption

models. Sample 3 was used for the BET tuning parameters in Case 3, the results for all four samples (Yu et al. 2014) are broken apart into adsorbed gas, free gas and OGIP at P90, P50 and P10 values in Table 5.

		Sample 1[a]		Sample 2		Sample 3		Sample 4		Literature[b]
Adsorption Model		**Langmuir**	**BET**	**Langmuir**	**BET**	**Langmuir**	**BET**	**Langmuir**	**BET**	**Langmuir**
Adsorbed Gas (Bcf/section)	P90	23	27	16	16	10	11	6	6	11
	P50	54	64	38	37	24	25	13	14	26
	P10	103	123	72	71	46	49	25	27	49
Free Gas (Bcf/section)	P90	4	1	8	8	11	11	14	13	11
	P50	16	11	23	24	30	29	35	34	29
	P10	44	36	56	57	67	66	76	75	66
OGIP (Bcf/section)	P90	30	32	26	26	23	23	20	20	23
	P50	72	77	63	62	55	55	49	49	56
	P10	142	153	125	125	112	113	100	101	113

[a] Samples 1-4 isotherm tuning parameters from Yu et al. 2014.
[b] Literature values from Dong et al. 2015.

Table 5. Select P-Values for Marcellus shale gas volumes calculated using Eq. (12) and Eq. (4). Isotherm tuning parameters are presented in Table 3.

*EUR and RF Prediction***.** Well configuration used in the semi-analytical model was similar to that of Dong et al. (2015), but the drainage region is infinite in this case study (**Table 6**). Also, an average pore diameter of 10 nm and the average diffusion coefficient of 1×10^{-5} m^2/s are assumed in this study based on Yu (2015). The semi-analytical model is not capable of accepting probabilistic inputs, and run-time would prevent a Monte Carlo simulation with a large number of samplings. A commercial software package of Design-Expert (Stat-Ease Incorporated, 2016) was used to generate 31 cases with discrete input parameters within the extrema conditions (**Table 7**) reported by Dong et al. (2015) and as combined in Appendix B. These parameters are used in the semi-analytical model to run the 31 selected cases for which cumulative production (EUR) obtained with the semi-analytical model are reported in **Figure 5**.

Input	**Marcellus**
Fracture Half-length (ft)	300
Lateral Length (ft)	3,700
Fracture Stages	12
Bottomhole Pressure (psi)	500

Table 6. Basic parameters used for each parameter in response surface mapping and values are from Dong et al. (2015).

Input	**Range**
Net Pay (ft)	45 - 384
Initial Pressure (psi)	2,000 - 5,100
Permeability (md)	0.2 - 0.9
Porosity (fraction)	0.03 - 0.13
Bulk Water Saturation (fraction)	0.06 - 0.53

Table 7. Extrema parameters used in response surface mapping; ranges are from Dong et al. (2015).

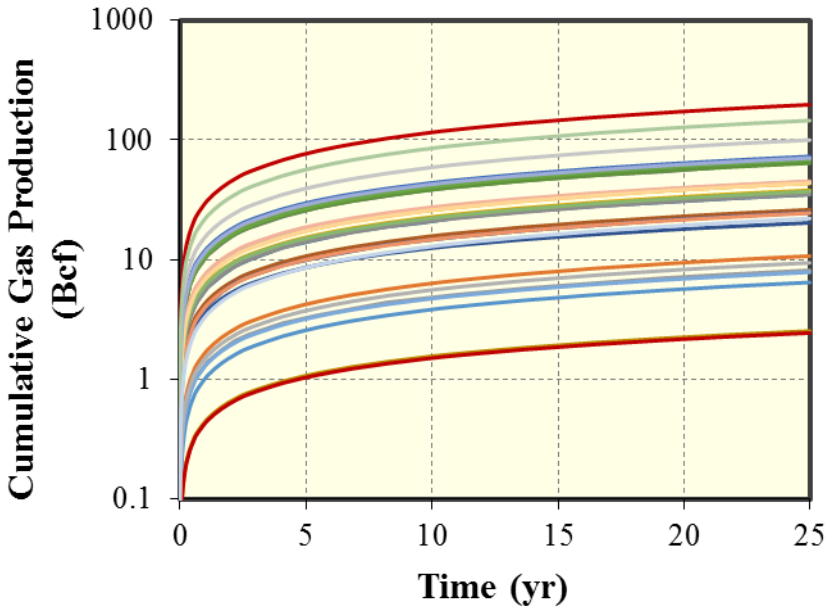

Figure 5. Production profiles output by the semi-analytical model for all 31 runs.

Eq. (22) was generated by Design-Expert to correlate 25-year cumulative production to key reservoir parameters. Figure 6 shows the EUR predicted by the RSM approach plotted against the independent EUR estimates from the semi-analytical model. The linear match in Fig. 6 validates mutual results [including Eq. (22)]. Units for the variables in Eq. (22) are specific and must be the same as the units used in Eq. (12). Although the reservoir behavior described by Eq. (22) was infinite acting, it was assumed that there was marginal drainage beyond 640 acres (1 section). This assumption was needed to generate RF from EUR and OGIP. The OGIP, EUR and RF distribution obtained from probabilistic simulation with @Risk are presented in **Figures 7-9** respectively and summarized in **Table 8**.

$$
\begin{aligned}
Log(EUR) = {} & -0.667562011 + 0.006044513\,h + 0.000410903\,P + 5.475553887\,\phi_b \\
& - 0.384706921\,S_{wb} + 384.0558206\,k - 4.3918 \times 10^{-8}\,h\,P + 0.00049401\,h\,\phi_b \\
& - 0.000339781\,h\,S_{wb} - 0.069247556\,h\,k + 8.44201 \times 10^{-5}\,P\,\phi_b + 1.64523 \times 10^{-5}\,P\,S_{wb} \\
& - 0.024383689\,P\,k - 6.158862192\,\phi_b\,S_{wb} - 3622.575768\,\phi_b\,k + 755.3728421\,S_{wb}\,k \\
& - 7.30711 \times 10^{-6}\,h^2 - 3.57571 \times 10^{-8}\,P^2 + 0.70870641\,\phi_b^2 + 0.008848315\,S_{wb}^2 \\
& + 9092.855716\,k^2 \quad . \qquad (22)
\end{aligned}
$$

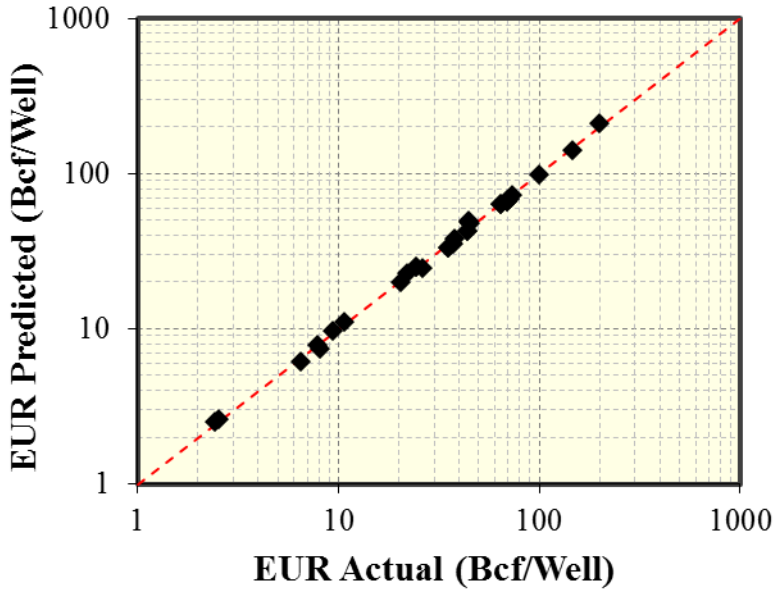

Figure 6. EUR (Bcf) per well predicted by RSM compared to EUR calculated by semi-analytical model.

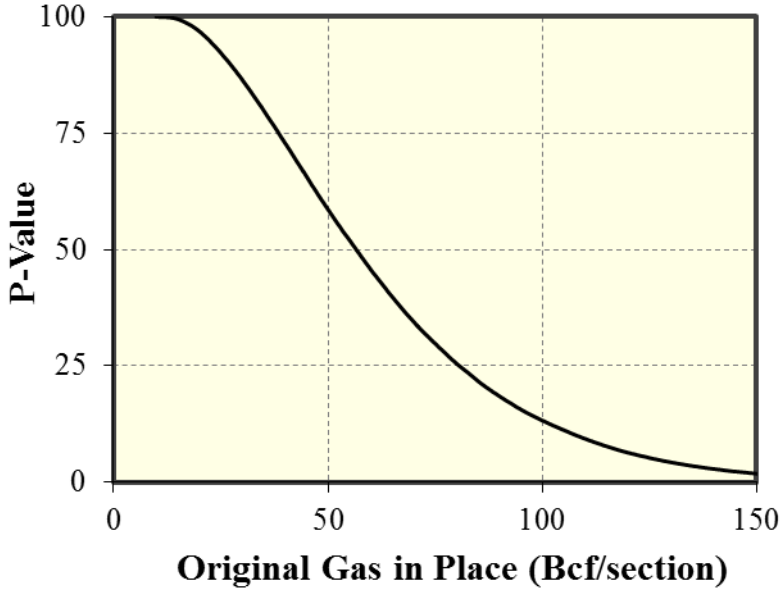

Figure 7. Probabilistic OGIP distribution for the Marcellus shale. Sample 3 BET tuning data was used for the adsorption model.

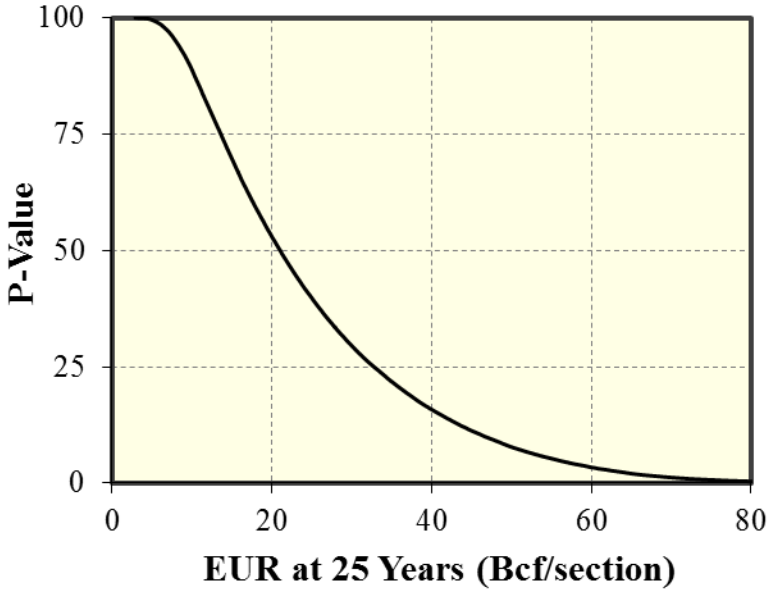

Figure 8. 25-Year EUR probabilistic distribution for the Marcellus shale determined from semi-analytical model.

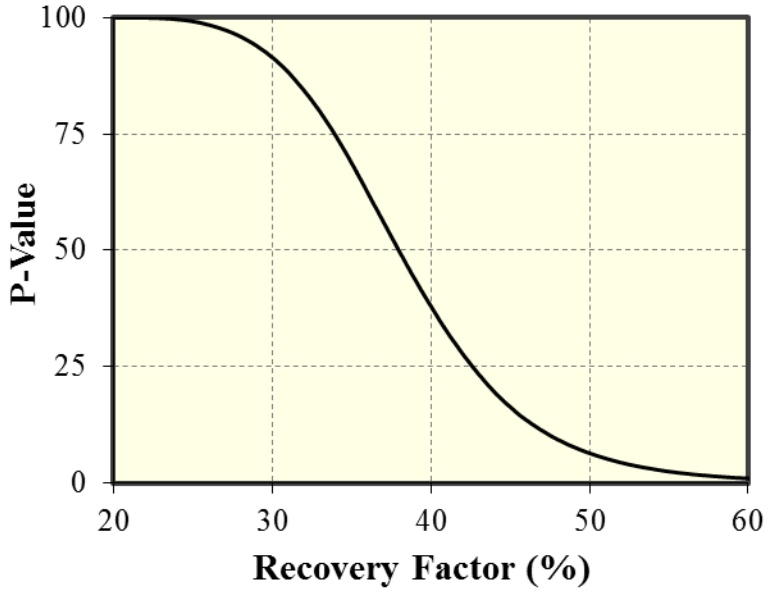

Figure 9. 25-year probabilistic percent recovery of OGIP for the Marcellus shale.

	OGIP (Bcf/section)	**EUR** (Bcf/Section)	**RF** (%)
P90	27.0	9.6	30.5
P50	56.3	21.0	38.0
P10	108.3	46.7	47.5

Table 8. Key P-values of 25-year percent recovery of OGIP for the Marcellus shale.

Discussion

Subtracting pore space occupied by adsorbed gas from pore space available for free gas results in a decrease in OGIP as compared to estimates of free gas in pore space plus adsorbed gas without taking into account the reduced space for free gas due to the presence of adsorbed gas (Table 2). Changing from a Langmuir isotherm to a BET isotherm had no clear trend in increasing OGIP. Based on the work of Yu et al. (2014), the high pressure (>3000psi) region where the models diverge, the BET isotherm has a greater estimated storage capacity than the Langmuir isotherm. Generally, the Langmuir isotherm serves as a minimum estimate of storage capacity although at sub-3000 psi pressures the BET isotherm may be marginally lower than the Langmuir isotherm when curve-fitting is based on lab data. The Langmuir isotherm could be seen as a lower limit to the estimate of adsorbed gas volume.

Lower Limit of BET Model. In the sample data provided by Yu et al. (2014) the Langmuir isotherm is fit to experimental data, and this approach displays artifacts in the results presented in Table 2. If the maximum number of adsorbed layers in the BET isotherm model is set to 1, the formula reduces to the same form as a Langmuir isotherm. Unless the adsorbed gas cannot form a complete layer, the Langmuir isotherm adsorbed gas volume should always be equal to or less than the BET isotherm. When fitting the Langmuir isotherm Yu et al. (2014) used as many data points as possible while still maintaining a good fit. The approach used is an excellent example of what a laboratory may obtain if they did not reach pressures great enough to notice a divergence from typical Langmuir behavior and served as a good comparison to the proper BET isotherm fit. The artifact of this is clearly seen in sample 2 in Table 5, where the BET adsorbed gas volume is less than the Langmuir isotherm. Any attempt to improve models from a lab derived Langmuir isotherm to a BET isotherm are expected to see similar results.

Upper Limit of BET Model. The tuning parameters used for the BET isotherm model in all samples are localized and not meant to be generalized to a large region. The extrapolation of a static BET model to a large region may produce a possibility of a negative free gas estimates (**Figure 11**).

The negative free gas in Figure 11 is easily quantified and explained. Due to the constraint of the pore space available, the adsorbed gas volume under reservoir conditions must also have an upper limit. At some critical value the pore space will be completely filled with adsorbed gas. Any increase beyond this critical value would result in a negative free gas estimate. The defining equation is derived in **Appendix C**:

$$v_a \leq \frac{\rho_a \, \phi_m \, (1 - S_w)}{\rho_b \, 1.318 \times 10^{-6} \, M} \quad . \tag{23}$$

If static tuning parameters are used for an isotherm model and are extrapolated to a larger region, a negative free gas volume may be produced due to violation of Eq. (23). The validity of extrapolating a Langmuir or BET isotherm model to a larger region will be dependent on scale. A drainage region could possibly be described by its neighbors tuning parameters, but extrapolation to the entire Marcellus is impossible without further work.

Negative free gas volumes were observed when the BET tuning parameters of samples 1 and 2 were used in the model. The results are thus invalid for a regional scale estimate. Sample 3 and 4 did not produce negative free gas volumes are more reliable. Sample 4 produced low estimates of adsorbed gas content, with a mean value of 44.6 scf/ton. Sample 3 produced a mean value of 80.6 scf/ton, which is closer to the values reported by Dong et al. (2015). For these reasons, sample 3 was used to generate Figure 4, and was also used for the semi-analytical model.

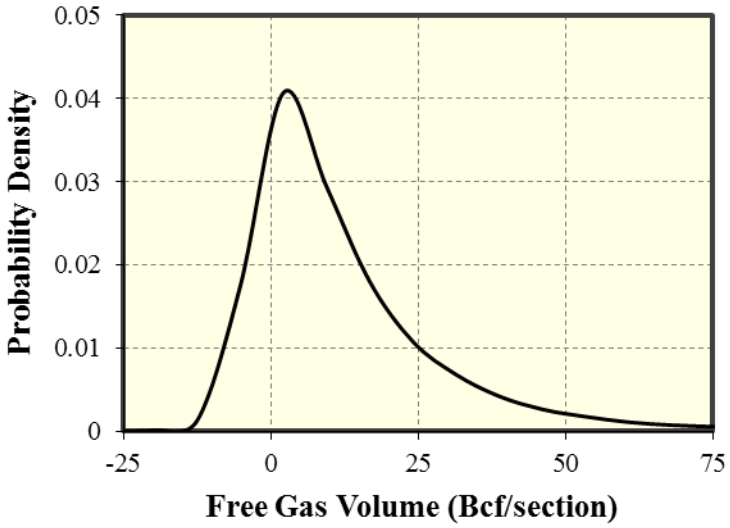

Figure 10. Free gas probability density function generated from sample 2 BET tuning.

Bounded Adsorbed Gas Volume. Due to the soft lower limit of the lab derived Langmuir isotherm, and the hard upper limit of the pore space, the adsorbed gas volume is well bounded.

$$v_{a\_Lang} \lesssim v_{a\_BET} \leq \frac{\rho_a \, \phi_m \, (1 - S_w)}{\rho_b \, 1.318 \times 10^{-6} \, M} \quad . \tag{24}$$

Compared to the Langmuir isotherm, the BET model is better connected with physical phenomena. The original BET paper (Brunauer et al. 1938), mentioned that the parameter C did not significantly depend on the surface being adsorbed to, but rather on the material adsorbing to the surface. The volume of one complete monomolecular layer, v_m is expected to correlate to surface area of the pore. Lastly, the maximum number of layers may correspond to a combination of surface area and pore space. It is expected that increasing surface area for a given pore volume would decrease the space available for multiple layers. Such relationships indicate that correlations to known reservoir data could be developed.

Comparison of Results. When adsorption is assumed to follow the Langmuir isotherm model, the Marcellus shale OGIP is 6-17% lower than the previously published 59 Bcf/section estimate (Dong et al 2015). The reduction of OGIP comes entirely from reduced free gas volume by the inclusion of adsorbed gas in the pore space. Changing from a Langmuir to a BET isotherm model caused up to a 7% increase in P50 OGIP. Negative free gas volumes were observed when the BET tuning parameters of samples 1 and 2 were used in the model. Despite being valid where the samples were taken, the occurrence of negative free gas volume indicates that such samples may not be applied in a regional scale estimation of OGIP. Samples 3 and 4 did not produce negative free gas volumes and therefore are considered more reliable in our application. P50 OGIP estimated using samples 3 and 4 BET isotherm data was 49-55 Bcf/section and is not notably different from the Langmuir isotherm model. Based on a 15 million acre land area (Dong et al. 2015) for the Marcellus, the new model estimates total P50 OGIP to be 1,137-1,297 Tcf. The new estimate is significantly lower than the 1,500 Tcf estimated by the U.S. Department of Energy (Ground Water Protection Council and ALL Consulting 2009). Our new OGIP estimation accounts for the reduction of pore space due to adsorbed gas which reduces the pore space available to free gas-in-place.

Using the EUR response surface model with sample 3 BET isotherm data, P50 OGIP and P50 EUR were 56 and 21 Bcf/section, and P50 RF was 38%. A slight difference in OGIP exists when coupled with the EUR model because the input distributions were slightly truncated. Total P50 OGIP estimate for the Marcellus for the coupled model was 1,320 Tcf, and P50 EUR was 492 Tcf. The EUR estimate is very close to the well-known Engelder-estimate of 489 Tcf (Engelder 2009).

Conclusions

A new model of shale original gas in place was created, which accounts for adsorbed gas volume in the pore space, new developments in gas adsorption behavior and a dual porosity model with various water saturations. A semi-analytical model was used to map EUR to key reservoir characteristics. Reservoir characteristics described by probability distributions were input into the OGIP and EUR models with Monte Carlo simulation. With probabilistic OGIP and EUR data, a RF distribution was obtained.

- Pore space competition between free gas and adsorbed gas volumes causes a 6-17% reduction of P50 OGIP in the Marcellus shale.
- Adsorbed gas volume is well bounded by the Langmuir isotherm estimation and the upper limit of pore space volume.
- Application of Langmuir and BET isotherm models to region scale models needs further developing.
- P50 EUR for the Marcellus shale was 492 Tcf, P50 RF was 38%.

When applied to a section with a standardized fracture spacing and certain fracture dimensions (Fig. 2) our method generates probabilistic OGIP, EUR, and RF estimates (Table 8) that may be used to pinpoint the good, bad and ugly producers.

Acknowledgements

We would like to express our gratitude for the financial support provided by the Crisman Institute for Petroleum Research which made this research possible.

Nomenclature

Bcf	=	Billion cubic feet
EUR	=	Estimated ultimate recovery
OGIP	=	Original gas in place
RF	=	Recovery factor
Tcf	=	Trillion cubic feet
A	=	Area of drainage region
B_g	=	Gas formation volume factor
C	=	Constant from net heat of adsorption
c_{frac}	=	Fracture compressibility
c_g	=	Isothermal gas compressibility factor
D_g	=	Fickian diffusivity coefficient
H	=	Height of pay zone
K	=	Permeability
K_n	=	Knudsen number
K_a	=	Differential equilibrium partitioning coefficient
M	=	Molecular weight of the gas
N	=	Maximum number of adsorbed gas layers
P	=	Pressure
P_0	=	Saturation pressure of the gas
P_{ST}	=	Stock tank pressure
S_g	=	Gas saturation
S_{wb}	=	Bulk water saturation
S_{wfrac}	=	Water saturation in fracture

S_{wm}	=	Water saturation in matrix
T	=	Temperature
T_{ST}	=	Stock tank temperature
V_a	=	Volume of adsorbed gas
V_f	=	Volume of free gas
v_a	=	Adsorbed gas volume
v_{a_BET}	=	Adsorbed gas volume from BET isotherm
v_{a_Lang}	=	Adsorbed gas volume from Langmuir isotherm
v_g	=	Gas velocity
v_{Lang}	=	Langmuir volume
Z	=	Gas compressibility factor
A	=	Constant
B	=	Non-Darcy Forchheimer coefficient
Δ	=	Dimensionless constrictivity factor
μ_g	=	Gas Viscosity
ρ_a	=	Density of adsorbed gas
ρ_g	=	Gas density
ρ_b	=	Bulk density of shale
T	=	Dimensionless Tortuosity
ϕ_a	=	Porosity occupied by adsorbed gas
ϕ_b	=	Bulk Matrix Porosity
ϕ_m	=	Matrix porosity
ϕ_f	=	Porosity created by fractures

SI Metric Conversion Factors

ft	×	3.048	×	10^{-1}	=	m
ft^3	×	2.832	×	10^{-2}	=	m^3
section	×	1			=	mi^2
psi	×	6.895			=	kPa
		(^{o}F-32)/1.8			=	^{o}C
		(^{o}R-491.67)/1.8			=	^{o}C

References

Abou-Kassem, J.H., Matter, L., Dranchuk, P.M. 1990. Computer Calculations of Compressibility of Natural Gas. J. Canadian Petrol. Tech. **29** (5): 105-108.

Alnoaimi, K.R., Kovscek, A.R. 2013. Experimental and Numerical Analysis of Gas Transport in Shale Including the Role of Sorption. Presented at the SPE Annual Technical Conference and Exhibition, New Orleans, Louisiana, 30 Sept - 2 October, SPE-166375-MS.

Ambrose, R. J., Hartman, R. C., Diaz-Campos, M. et al. 2012. Shale Gas-in-Place Calculations Part 1: New Pore-Scale Considerations. SPE J. **17** (1): 219–229. SPE-131772-PA.

Brunauer, S., Emmet, P.H., and Teller, E., 1938. Adsorption of Gases in Multimolecular Layers. J. Am. Chem. Soc. **60**: 309-319.

Clarkson, C.R., Bustin, R.M., and Levy, J.H. 1997. Application of the Monolayer/Multilayer and Adsorption Potential Theories to Coal Methane Adsorption Isotherms at Elevated Temperature and Pressure. Carbon **35** (12): 1689-1705.

Dong, Z. 2012. A New Global Unconventional Natural Gas Resource Assessment. Dissertation, Texas A&M University, College Station, Texas, August 2012.

Dong, Z., Holditch, S.A., McVay, D.A., Ayers, W.B. 2015. Probabilistic Assessment of World Recoverable Shale-Gas Resources. SPE-167768-PA.

Engelder, T. 2009. Marcellus 2008: Report card on the breakout year for gas production in the Appalachian Basin. Fort Worth Basin Oil and Gas magazine, August 2009 edition, Abilene, TX: pp. 18-22.

Evans, R.D., and Civan, F. 1994. Characterization of Non-Darcy Multiphase Flow in Petroleum Bearing Formations. *Report. U.S. DOE Contract No. DE-AC22-90BC14659, School of Petroleum and Geological Engineering*, University of Oklahoma.

Ground Water Protection Council, ALL Consulting. 2009. Modern Shale Gas. Development in the United States: A Primer. U.S. Department of Energy, Office of Fossil Energy, National Energy Technology Laboratory.

Jin, Z., Firoozabadi, A. 2016. Thermodynamic Modeling of Phase Behavior in Shale Media. SPE-176015-PA.

Langmuir, I. 1918. The Adsorption of Gases on Plane Surfaces of Glass, Mica and Platinum. J. Am. Chem. Soc. **40**: 1361–1403.

Loucks, R.G., Reed, R.M., Ruppel, S.C., and Jarvie, D.M. 2009. Morphology, Genesis, and Distribution of Nanometer-Scale Pores in Siliceous Mudstones of the Mississippian Barnett Shale. J. Sediment. Res. **79**: 848-861.

Myers, R. H., Montgomery, D. C., and Anderson-Cook, C. 2008. Response Surface Methodology: Process and Product Optimization Using Designed Experiments, 3rd Edition, New York, John Wiley and Sons.

Naraghi, M.E., Javadpour, F. 2015. A Stochastic Permeability Model for the Shale-Gas Systems. Int. J. Coal Geol. **140**: 111-124.

Ozdemir, E. 2004. *Chemistry of the Adsorption of Carbon Disoxide by Argonne Permium Coals and a Model to Simulate CO_2 Sequesteration in Coal Seams*. PhD dissertation, University of Puittsburgh (September 2004)

Riewchotisakul, S. and Akkutlu, I. Y. 2015. Adsorption Enhanced Transport of Hydrocarbons in Organic Nanopores. Presented at the SPE Annual Technical Conference and Exhibition, Houston, Texas, 28–30 September, SPE-175107-MS.

Sondergeld, C.H., Ambrose, R.J., Rai, C.S. and Moncrieff, J. 2010. Micro-Structural Studies of Gas Shales. Presented at the SPE Unconventional Gas Conference held in Pittsburgh, Pennsylvania, USA, 23-25 February, SPE-131771-PA.

Stat-Ease, Inc. 2016. Design-Expert® 10 User's Guide.

Wang, F.P., Reed, R.M. 2009. Pore Networks and Fluid Flow in Gas Shales. Presented at the Annual Technical Conference and Exhibition, SPE, New Orleans, Louisiana. 4-7 October, SPE-124253-MS.

Yu, W., 2015. A Comprehensive Model for Simulation of Gas Transport in Shale Formation with Complex Hydraulic Fracture Geometry. Presented at SPE Annual Technical Conference and Exhibition, Houston, Texas, 28-30 September. SPE-2015-178747-STU.

Yu, W., and Sepehrnoori, K. 2014. An Efficient Reservoir Simulation Approach to Design and Optimize Unconventional Gas Production. J. Can. Pet. Technol. **53**: 109-121.

Yu, W., Sepehrnoori, K., and Patzek, T.W. 2014. Modeling Gas Adsorption in Marcellus Shale Using Langmuir and BET isotherms. Presented at the SPE Annual Technical Conference and Exhibition, Amsterdam, The Netherlands, 27-29 October, SPE-170801-MS.

Yu, W., Wu, K., and Sepehrnoori, K. 2016. A Semianalytical Model for Production Simulation from Nonplanar Hydraulic-Fracture Geometry in Tight Oil Reservoirs. SPE J. **21** (3): 1028-1040.

Appendix A – Dong et al. (2015) Model and Probabilistic Inputs

In addition to our evaluation of the Marcellus shale in the main text, the model for Case 3 (Figure 1B) was applied to reassess the OGIP estimates of all major US shale gas regions (Barnett, Eagle Ford, Fayetteville, Haynesville) considered in Dong et al. (2015). Our review is included purely for the reader's interest, and an in-depth analysis other than a comparison of the principal results has not been attempted. The static inputs used are in **Table A-1**, and probabilistic inputs used are in **Table A-2**. Distribution output is shown in **Figure A-1**.

Input	Barnett	Eagle Ford	Fayetteville	Haynesville
Area (acres)	640	640	640	640
Temperature (˚R)	665	660	585	785
Bulk Rock Density (g/cc)	2.5	2.5	2.5	2.5
Storativity Ratio	0.1	0.1	0.1	0.1
Specific Gravity	0.62	0.6	0.58	0.58

Table A-1. Static values (Dong et al. 2015) used to calculated gas volumes and production forecasts.

Input	Barnett	Eagle Ford	Fayetteville	Haynesville
Net Pay (ft)	Log-normal[a] (200, 50)	Log-normal (130, 50)	Log-normal (150, 50)	Log-normal (200, 80)
Initial Pressure (psi)	Uniform[b] (3000, 5000)	Log-normal (7,200, 1,000)	Triangular[e] (800, 3,100, 4,000)	Uniform (7,00, 10,000)
Permeability (md)	Log-normal (0.0005, 0.0005)	Log-normal (0.0004, 0.001)	Log-normal (0.002, 0.00005)	Log-normal [0.034, 0.032, Shift(-0.001)]
Porosity (fraction)	Uniform (0.04, 0.05)	Inv-Gauss[c] (0.1, 6.8)	Log-normal (0.08, 0.02)	Log-normal (0.126, 0.03)
Bulk Water Saturation (fraction)	Uniform (0.25, 0.05)	Gamma[d] [3.8, 0.3, Shift(0.06)]	Uniform (0.15, 0.35)	Uniform (0.16, 0.41)

[a] Log-normal (mean, standard deviation)
[b] Uniform (min, max)
[c] Inv-Gauss (mean, shape parameter)
[d] Gamma (shape parameter, scale parameter)
[e] Triangular (min, most likely, max)

Table A-2. Distribution functions (Dong et al. 2015) used to calculated gas volumes and production forecasts.

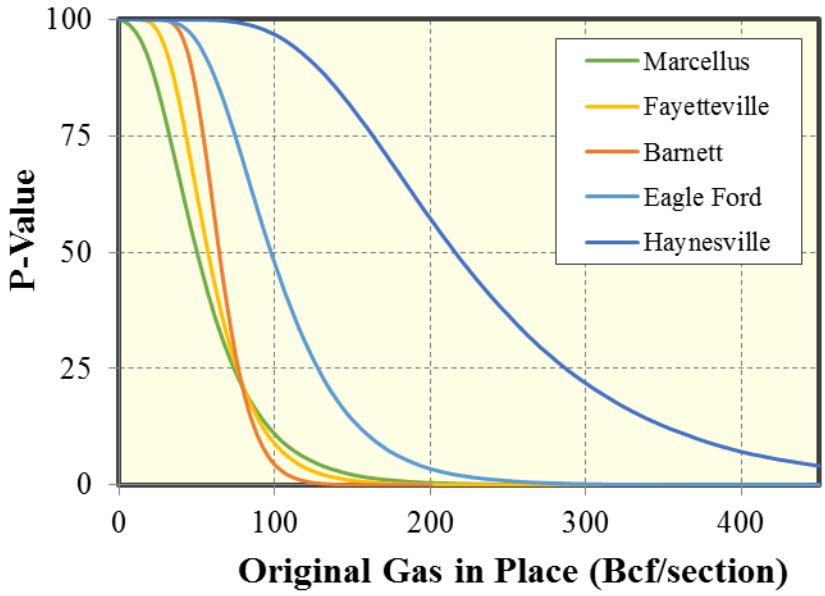

Figure A-1. Static values (Dong et al. 2015) used to calculated gas volumes and production forecasts.

Based on the information in Dong (2012) the OGIP model used was reconstructed. Eqs. (A-1) to (A-5) are the same as Eqs. (1), (6), (13), (2) and (3) respectively from the methods presented earlier.

$$OGIP = V_f + V_a \quad . \tag{A-1}$$

$$V_f = 43560 \frac{A\, h\, \phi_b (1 - S_w)}{B_g} \quad . \tag{A-2}$$

$$B_g = Z \frac{T\, P_{sc}}{P\, T_{sc}} \quad . \tag{A-3}$$

$$V_a = 1359.7\, A\, h\, \rho_b v_a \quad . \tag{A-4}$$

$$v_{a\_Lang} = V_L \left(\frac{P}{P + P_L} \right) \quad . \tag{A-5}$$

The only value not clearly defined in Dong (2012) was the calculation of Z factor. In our study, the conventional method of calculating Z factor was used, as outlined in methods, for both the new model and the recreation of Dong et al. (2015). This approach allowed us to independently reproduce and confirm the results by Dong et al. (2015) for the Barnett, Marcellus, Fayetteville and Haynesville shales. However, we were unable to match the prior results of Dong et al. (2015) for the Eagle Ford shale (**Table A-3**). Our evaluation gives a P50 OGIP of 102 Bcf/section, whereas 59 Bcf/section was reported by Dong et al. (2015). As stated in the methods, the probabilistic values published in Dong et al. (2015) were used. The published parameter distribution for Barnett shale porosity had a mean of 0.004, but earlier in the same paper the range had been listed as 0.04 to 0.05. The distribution published in Dong (2012) used a mean of 0.04 for porosity with the distribution for all other parameters remaining constant. The mean of 0.004 is likely a typo and thus a mean of 0.04 was used in this paper. The distribution functions are defined in Table A1, with the corrected Barnett mean porosity.

		Barnett	Eagle Ford	Marcellus	Fayetteville	Haynesville
OGIP	P50[a]	70	59	59	79	206
(Bcf/section)	P50[b]	74	102	59	78	211

[a] P50 OGIP values as published by Dong et al. 2015

[b] P50 OGIP values as reproduced using Dong et al. 2015 OGIP model and inputs as detailed in Appendix A.

Table A-3. Comparison of P-Values published by Dong et al. (2015), and results using their inputs with a recreation of their model.

Dong et al. (2015) mentions that the distributions used in Table A1 are not unique, they are outputs to 2-year cumulative production matching with an analytical production model. How other non-unique outputs from the model influence the calculated OGIP was not attempted in the original analysis nor in the present study. Based on another set of solutions, the distribution for Haynesville pay height (in ft) changed from Log-normal (200, 80) to Log-normal (130, 80) (personal communication by Dong). According to the method published by Dong et al., (2015) the distribution with a mean pay height of 130 ft would be excluded because it falls outside of the acceptable range of 200-300 ft. However, this example illustrates how the output can vary drastically based on certain assumptions and constraints adopted. The non-uniqueness to the distributions may be an explanation for the mismatch between published and reproduced Eagle Ford OGIP (Table A-3). One set of distributions may have been presented, and another used to calculate OGIP. While the models presented herein are a combination of the best and most recent developments in the field, the inputs may still be more uncertain that they initially appear.

Appendix B – RSM Model Data

Run	h (ft)	P (psi)	ϕ_b	S_{wb}	k (10^{-3} md)	EUR (Bcf/well)
1	138	4,015	0.12	0.23	0.20	35.2
2	172	3,659	0.13	0.53	0.42	26.1
3	384	3,535	0.07	0.30	0.52	64.1
4	45	2,000	0.03	0.15	0.20	2.5
5	296	2,915	0.03	0.53	0.20	20.3
6	384	5,100	0.13	0.06	0.32	197.6
7	216	5,100	0.09	0.30	0.90	68.6
8	384	2,000	0.12	0.06	0.20	69.2
9	138	4,015	0.12	0.23	0.20	35.2
10	384	2,000	0.03	0.07	0.90	38.0
11	215	2,062	0.13	0.31	0.58	24.5
12	384	3,535	0.07	0.30	0.52	64.1
13	45	2,000	0.10	0.08	0.90	6.5
14	45	4,325	0.03	0.12	0.90	10.7
15	92	2,093	0.04	0.49	0.76	8.1
16	244	3,550	0.07	0.53	0.87	44.2
17	367	5,100	0.13	0.53	0.32	72.9
18	216	5,100	0.09	0.30	0.90	68.6
19	45	5,100	0.05	0.50	0.35	7.9
20	215	2,062	0.13	0.31	0.58	24.5
21	45	3,752	0.13	0.53	0.87	9.4
22	211	3,411	0.07	0.06	0.53	43.7
23	281	2,605	0.08	0.23	0.90	44.8
24	384	2,000	0.10	0.53	0.90	37.2
25	45	2,000	0.11	0.53	0.20	2.4
26	296	5,100	0.06	0.43	0.20	45.2
27	384	5,100	0.03	0.53	0.90	100.1
28	211	3,411	0.07	0.06	0.53	43.7
29	384	5,100	0.03	0.06	0.20	70.7
30	384	3,922	0.13	0.06	0.90	145.7
31	45	5,100	0.13	0.06	0.62	22.1

Table B-1. Input and output values for each run of the semi-analytical model.

Appendix C – Upper Limit of Adsorbed Gas Volume

Pore space occupied by the adsorbed gas is defined in terms of the volume of adsorbed gas (v_a), bulk rock density (ρ_a), bulk rock density (ρ_b), and molecular weight (M) (Ambrose et al. 2012):

$$\phi_a = 1.318 \times 10^{-6} M \frac{\rho_b}{\rho_a} v_a \quad . \tag{C-1}$$

When porosity occupied by adsorbed gas (ϕ_a) is greater than the free gas volume the model is no longer valid because an illogical result has been produced: negative free gas volume. This is the only limitation placed on the model, the pore space occupied by the adsorbed gas must be less than or equal to the pore space occupied by free gas:

$$\phi_a \leq \phi_m (1 - S_w) \quad . \tag{C-2}$$

Combining the two Eqs. (C-1) and (C-2):

$$1.318 \times 10^{-6} M \frac{\rho_b}{\rho_a} v_a \leq \phi_m (1 - S_w) \quad . \tag{C-3}$$

Solving Eq. (C-3) for ρ_a results in the following equation:

$$\rho_a \geq \frac{v_a \rho_b 1.318 \times 10^{-6} M}{\phi_m (1 - S_w)} \quad . \tag{C-4}$$

or in terms of free gas volume:

$$v_a \leq \frac{\rho_a \phi_m (1 - S_w)}{\rho_b 1.318 \times 10^{-6} M} \quad . \tag{C-5}$$

Given a volume of adsorbed gas, there exists a critical density that will cause adsorbed gas to expand to fill the pore space within the shale. A density below the critical value defined by Eq. (C-4), or a volume defined by Eq. (C-5) is physically possible only if some or all of adsorbed gas located in the matrix outside of the pore space.